Numerical Simulation for Performance Study of Solar Chimney.

M. Mousa
Professor and head Mechanical Power Engineering Dept., Faculty of Engi-neering, Monsoura University, Monsoura, Egypt

Ahmed Hegazi
Lecturer, Mechanical Power Engineering Dept., Faculty of Engineering, Monsoura University, Monsoura, Egypt, ahmedabd-elsallam@gmail.com

M. Abd Rabou
B.Sc Mechanical Power Engineering, Faculty of Engineering, Monsoura University, Monsoura, Egypt

Numerical Simulation for Performance Study of Solar Chimney
المحاكاة العددية لدراسة أداء مدخنة شمسية

M. G. Mousa[1], A.A.Hegazi[2] and M.M.Abd Rabou[3]

[1] Professor and head Mechanical Power Engineering Dept., Faculty of Engineering, Monsoura University, Monsoura, Egypt

[2] Lecturer, Mechanical Power Engineering Dept., Faculty of Engineering, Monsoura University, Monsoura, Egypt

[3] B.Sc Mechanical Power Engineering, Faculty of Engineering, Monsoura University, Monsoura, Egypt

الملخص

في هذه الدراسة نقوم بدراسة التدفق الحرارى الحر فى مدخنة شمسية ذات أبعاد ثنائية. ويستخدم النموذج للحصول على تأثيرالمعاملات التى لها التأثير على أداء المدخنة الشمسية. وتم داسة وتحليل السريان والحرارة داخل المدخنة لقيم مختلفة لعدد رايلى تتراوح بين ($10^3≤Ra≤10^6$) ، نسبة الارتفاع تتراوح خلال (X≤1 / 0.25≤Y) وسرعة اللابعدية لدخول الهواء المدخنة تتراوح بين(0.5≥Uin≥0) مع ثبات عدد برانتدل($Pr = 0.7$) ومعامل قوس المدخنة (R=0.04) . تحل المعادلات التي تحكم مع تقنية الفروق المحدودة باستخدام نظام الفرق المركزي. تم استخدام برنامج كمبيوتر (Matlab2012) لتنفيذ الحل العددي. ثم تقدم اشكال خطوط السريان وخطوط الحرارة وتقييم أيضاً أداء محطات المدخنة الشمسية في مدينة الوادي الجديد في مصر وحساب تقديري لكمية الطاقة الكهربائية المولدة منها.

Abstract

In the present study, the problem of the two-dimensional steady free convection flow in solar chimney. The present model is utilized to obtain the results of the effect of parameters, which influence the performance of solar chimney. The problem investigates the streamline and isothermal inside the chimney for Rayleigh numbers ranging within ($10^3 ≤Ra≤10^6$), aspect ratio ranging within ($0.25≤Y/X≤1$) and inlet velocity ($0≤U_{in}≤0.5$) for a fixed Prandtl number ($Pr=0.7$) and coefficient of arc (R=0.04). The governing equations are solved with finite-difference technique by central difference scheme. A computer program in (Matlab2012) was used to carry out the numerical solution. The results are presented in the form of streamline and isotherm plots. Also, the performance of solar chimney power plants at New Village city in Egypt is evaluated and an approximation of the quantity of the generated electrical energy is estimated.

Keywords

Nomenclature

c_p	Specific heat at constant pressure	$J.kg^{-1}.K^{-1}$		ficient of arc, (R=X*Y)	
H	Chimney height	m		Rayleigh number, (	
K	Thermal conductivity	$W.m^{-1}.K^{-1}$	Ra	$\frac{g\beta qL^4}{\alpha \upsilon K}$)	------
L	Radius of collector	m	T	Temperature	K
Pr	Prandtl number, (υ / α)	------	u,v	Velocity components in Cartesian coordinates	$m.s^{-1}$
q	Solar radiation	$W.m^{-2}$	U, V	Dimensionless velocity components in	------
R	Dimensionless coef-	------			

	Cartesian coordinates	
V_{max}	Dimensionless maximum velocity	------
x, y	Cartesian coordinates	m
X, Y	Dimensionless Cartesian coordinates	------
ΔX	Dimensionless mesh size	------

Greek symbols

α	Thermal diffusivity	m².s⁻¹
α_g	Collector ground absorbance	------
β	Thermal expansion coefficient	K⁻¹
Θ	Dimensionless temperature, $((T-T_a)/(q.K/L))$	------
Θ_{max}	Maximum dimensionless temperature	------
μ	Dynamic viscosity	kg.m⁻¹.s⁻¹
v	Kinematic viscosity, (μ/ρ)	m².s⁻¹
ρ	Density	kg.m⁻³
ω	Vorticity	s⁻¹
Ω	Dimensionless vorticity, $(\omega.L^2/\alpha)$	------
ψ	Stream function	m².s⁻¹
Ψ	Dimensionless stream function, (ψ/α)	------

Subscripts

a	Ambient
C	Collector
g	Ground of collector
in	Inlet
max	Maximum
min	Minimum
s	Solar

Abbreviations

CFD	Computational Fluid Dynamics
SCPP	Solar Chimney Power plant

Introduction

Solar energy is a renewable and clean energy resource, which produces neither greenhouse effect gases nor hazardous wastes through its utilization. Of many techniques utilizing solar energy, solar power generation seems to be one of the most attractive. Electric power can be obtained from solar energy by two means, photovoltaic effect and solar thermal generator. Solar cells form a semiconductor unit to produce electric current based on photovoltaic effect, and the solar thermal generator, is always driven by steam generated by large scale solar concentrator.

A solar chimney power plant (SCPP) combines the concept of solar air collector and central updraft chimney to generate a solar induced convective flow which drives wind turbines to generate electricity. The SCPP consists of a greenhouse roof collector and updraft chimney that is located at the centre of the greenhouse roof collector. The greenhouse roof collector is usually made of plastic sheet or glass plate which traps the solar energy and elevates the air temperature. The chimney is used to direct and vent the hot air through the wind turbine. The wind turbine is used to convert the air kinetic energy into mechanical work. The main advantages of a solar chimney system are the low maintenance cost, the simplicity of operation and the durability of the system.

Literature review

Haaf et al. [1] provided fundamental studies for the Spanish prototype in which the energy balance, design criteria and cost analysis were discussed and reported preliminary test results of the solar chimney power plant.

Schlaich et al. [2] presented theory, practical experience, and economy of solar chimney power plant to give a guide for the design of 200 MW commercial solar chimney power plant systems.

Zhou et al. [3] provided a comprehensive picture of research and development of solar chimney power technology

in the past few decades. The description, physical process, experimental and theoretical study status, and economics for the conventional solar chimney power technology are included as well as descriptions of other types of SC power technology.

Bernardes et al. [4] presented a theoretical analysis of a solar chimney, operating on natural laminar convection in steady state. In order to predict thermo-hydrodynamic behavior of air, temperature conditions were imposed on entrance, so as to guarantee steady laminar flow along the device. The mathematical model was analyzed by the method of Finite volumes in generalized coordinates. Velocity field and temperature distribution in the flow were obtained under imposed thermal conditions.

Huang et al. [5] established a Solar Chimney Power Plant System (SCPPS) used to experimental research for being a large scale system. Using the Spanish prototype plant as simulation object, the SCPPS is numerical simulation calculated for performance.

Tahar and Mahfoud [6] presented a numerical study of natural convection in a solar chimney. The transported fluid is the air (Pr=0.702), it is considered as a Newtonian and incompressible fluid, by using the Boussinesq approximation, the governing equations are taken to be in the vorticity-stream function formulation in hyperbolic coordinates. For heating conditions, isothermal walls of the collector were supposed.

Mostafa et al. [7] presented mathematical model and governing equations of solar chimney to improve the performance of solar chimney under effects of various parameters, and study of possibility of installing solar chimney in Egypt. The mathematical simulation of the solar chimney has been developed including all its performance parameters, dimensions (collector, chimney and turbine) and the metrological data; which were considered as inputs of the simulation program.

Hamdan [8] presented a mathematical thermal model for steady state airflow inside a solar chimney power plant using modified Bernoulli equation with buoyancy effect and ideal gas equation. The study evaluates the use of constant density assumption across the solar chimney and compares it with more realistic chimney mathematical discrete model that allows density variation across the chimney.

Scope of the Present Work

Numerical simulation of the performance of flow inside solar chimney effect by operating parameter such as Rayleigh number ranging within ($10^3 \leq Ra \leq 10^6$), aspect ratio ranging within ($0.25 \leq Y/X \leq 1$) and inlet velocity and inlet velocity ($0 \leq U_{in} \leq 0.5$) in solar chimney performance as well as evaluate the electrical energy production in New Vellage city of Egypt using the solar chimney.

System description

A typical solar chimney power plant consists of a collector, chimney and turbine as shown in Fig. 1, heat flux heating the air by solar radiation and the natural ground below it form a hot air collector.

A vertical chimney with large air inlets at its base. The joint between the cover and the chimney base is airtight. As hot air is lighter than cold air it rises up the chimney. Suction from the chimney then draws in more hot air from the collector, and cold air enters from the outer perimeter. Thus, solar radiation causes a constant updraught in the chimney. The energy that the hot air contains is converted into mechanical energy by pressure staged wind turbines at the base of the chimney, and into electrical energy conventional generators.
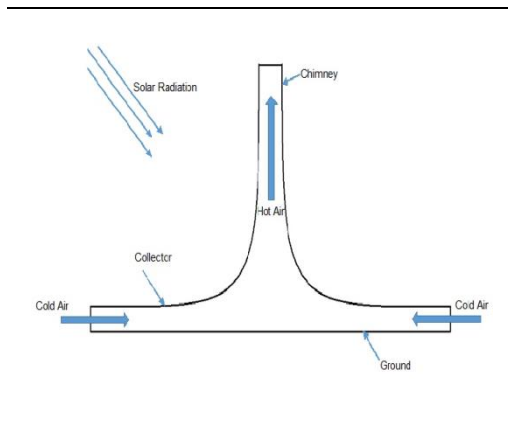
Fig. 1 Schematic diagram of a solar chimney power plant

Mathematical Modeling and assumption

A mathematical model of the natural buoyancy-driven fluid flow and heat transfer in the solar chimney shown in Fig. 2 have been adopted. The following assumptions have been used to simplify the governing equations. The fluid is assumed to be Newtonian, steady and incompressible and the thermo physical properties are assumed to be constant. The air flow in the system is due to buoyancy force in solar chimney, the profile of velocity is uniform at the inlet, and Mach number for air is below 0.3. The radiation heat transfer is negligible. The ground absorbance is $\alpha_g=$ 0.5[9] and all physical properties are evaluated in the ambient temperature.
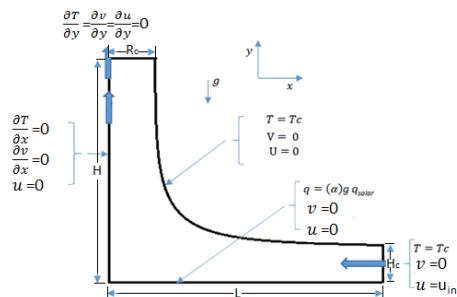
Fig. 2 Schematic diagram problem study and boundary conditions

Governing Equation

The equations in two-dimensional Cartesian coordinates (x, y), the Navier–Stokes equations for steady laminar natural convection flow using conservation of mass, momentum and energy equation within the framework of the Boussinesq approximation can be written as:

$$\frac{\partial u}{\partial x} + \frac{\partial v}{\partial y} = 0 \tag{1}$$

$$u\frac{\partial u}{\partial x} + v\frac{\partial u}{\partial y} = \upsilon(\frac{\partial^2 u}{\partial x^2} + \frac{\partial^2 u}{\partial y^2}) \tag{2}$$

$$u\frac{\partial v}{\partial x} + v\frac{\partial v}{\partial y} = \upsilon\left(\frac{\partial^2 v}{\partial x^2} + \frac{\partial^2 v}{\partial y^2}\right) - g\beta(T - T_a) \tag{3}$$

$$u\frac{\partial T}{\partial x} + v\frac{\partial T}{\partial y} = \alpha(\frac{\partial^2 T}{\partial x^2} + \frac{\partial^2 T}{\partial y^2}) \tag{4}$$

Equations (1 to 4) are the continuity, x-momentum, y-momentum, and energy equations, respectively. The above equations are solved using the boundary conditions:

At roof of the collector $R = L \cdot H$
$$u = v = 0; \ \ T = T_a \tag{5}$$
At axis of symmetry (x = 0, 0 ≤ y ≤ H)
$$\frac{\partial v}{\partial x} = 0 \ ; u = 0; \ \ \frac{\partial T}{\partial x} = 0 \tag{6}$$
At ground (y = 0, 0 ≤ x ≤ L)
$$u = v = 0; \ q = (\alpha)_g \cdot q_s \tag{7}$$
At collector inlet (x = L, 0 ≤ y ≤ R_C)
$$v = 0; \ u = u_{in}; \ T = T_a \tag{8}$$
At chimney outlet (y = H, 0 ≤ x ≤ H_c)
$$\frac{\partial u}{\partial y} = \frac{\partial v}{\partial y} = 0; \ \ \frac{\partial T}{\partial y} = 0 \tag{9}$$

Solving the governing equations (1 to 4) with their boundary conditions equations (5 to 9), therefore, the velocity and temperature distributions throughout the flow field can be obtained.

Simplified form of governing equations

The governing equations, i.e., equations (1 to 4), are given in terms of the so-called primitive variable, i.e., u and v. The solution procedure discussed here is based on equations involving the function, ψ, the vorticity, ω, and the temperature, T, as variables. The stream function and vorticity are defined by:

$$u = \frac{\partial \psi}{\partial y} \tag{14}$$

$$v = -\frac{\partial \psi}{\partial x} \tag{15}$$

$$\omega = \left(\frac{\partial v}{\partial x} - \frac{\partial u}{\partial y}\right) \tag{16}$$

The vorticity equation is obtained by taking the y-derivative of Eq. (2) and subtraction from it the x-derivative of Eq. (3). Using the definition of vorticity and the continuity equation, this equation can be written as:

$$\frac{\partial \psi}{\partial y}\frac{\partial \omega}{\partial x} - \frac{\partial \psi}{\partial x}\frac{\partial \omega}{\partial y} = \upsilon \left(\frac{\partial^2 \omega}{\partial x^2} + \frac{\partial^2 \omega}{\partial y^2}\right) + g\beta \frac{\partial T}{\partial x}$$

$$(17)$$

According to the forgoing definition (16), the voracity ω can be expressed in term of stream function ψ as:

$$\omega = -\left(\frac{\partial^2 \psi}{\partial x^2} + \frac{\partial^2 \psi}{\partial y^2}\right) \qquad (18)$$

With the aid of the definition of stream function (14 and 15), the energy equation (4) takes the following form:

$$\frac{\partial \psi}{\partial y}\frac{\partial T}{\partial x} - \frac{\partial \psi}{\partial x}\frac{\partial T}{\partial y} = \alpha \left(\frac{\partial^2 T}{\partial x^2} + \frac{\partial^2 T}{\partial y^2}\right) \qquad (19)$$

Equations (17 to 19) are converted to dimensionless equations by using dimensionless variables:

$$X = \frac{x}{L}; Y = \frac{y}{L}; U = \frac{uL}{\alpha}; V = \frac{vL}{\alpha}; \Psi = \frac{\psi}{\alpha}$$
$$\Omega = \frac{\omega L^2}{\alpha} \ and \ \theta = \frac{T - T_a}{(q\,L/k)} \qquad (20)$$

where X,Y,U,V,θ,Ψ and Ω are the dimensionless horizontal coordinate, vertical coordinate, velocity component in horizontal direction, velocity component in vertical direction, temperature, stream function, and vorticity, respectively. Substitution with the above dimensionless expression of dependent and independent variables (20) into equations (17 to 19). The dimensionless forms of the momentum, vorticity and energy equation can be written as:

$$\frac{\partial \Psi}{\partial Y}\frac{\partial \Omega}{\partial X} - \frac{\partial \psi}{\partial X}\frac{\partial \Omega}{\partial Y} = Pr\left(\frac{\partial^2 \Omega}{\partial X^2} + \frac{\partial^2 \Omega}{\partial Y^2}\right) + $$
$$RaPr\frac{\partial \theta}{\partial X} \qquad (21)$$
$$\Omega = -\left(\frac{\partial^2 \Psi}{\partial X^2} + \frac{\partial^2 \Psi}{\partial Y^2}\right) \qquad (22)$$
$$\frac{\partial \Psi}{\partial Y}\frac{\partial \theta}{\partial X} - \frac{\partial \Psi}{\partial X}\frac{\partial \theta}{\partial Y} = \frac{\partial^2 \theta}{\partial X^2} + \frac{\partial^2 \theta}{\partial Y^2} \qquad (23)$$

where the dimensionless numbers, the Prandtl and Rayleigh numbers are defined as follows,

$$Ra = \frac{g\beta qL^4}{\alpha \upsilon k} \ and \ Pr = \frac{\upsilon}{\alpha} \qquad (24)$$

According to the dimensionless variables, the boundary conditions for the governing equations are specified as follows:

At roof of the collector ($R = X \cdot Y$)

$$\Psi = 0; \ \frac{\partial \Psi}{\partial Y} = \frac{\partial \Psi}{\partial X} = 0; \ \theta = 0 \qquad (25)$$

At axis of symmetry (X = 0, $0 \le Y \le$ H/L)

$$\frac{\partial^2 \Psi}{\partial X^2} = 0 \ ; \frac{\partial \Psi}{\partial Y} = 0; \ \frac{\partial \theta}{\partial X} = 0 \qquad (26)$$

At ground (Y = 0, $0 \le X \le 1$)

$$\frac{\partial \Psi}{\partial Y} = -\frac{\partial \Psi}{\partial X} = 0; \ \frac{\partial \theta}{\partial Y} = -\alpha_g \qquad (27)$$

At collector inlet (X = 1, $0 \le Y \le$ R$_C$/L)

$$-\frac{\partial \Psi}{\partial X} = 0; \ \frac{\partial \Psi}{\partial Y} = U_{in}; \ \theta = 0 \qquad (28)$$

At chimney outlet (y = H/L, $0 \le X \le$ H$_c$/L)

$$\frac{\partial^2 \Psi}{\partial Y^2} = \frac{\partial^2 \Psi}{\partial X^2} = 0; \ \frac{\partial \theta}{\partial Y} = 0 \qquad (29)$$

Equations (21 to 23) are converted to linear algebraic equations.

Results and discussion

To solve this system of equations with associated boundary conditions equations, an iterative finite difference solution procedure is used. The method of numerical solution taken is the central finite difference scheme which is for the discretization technique to convert the partial differential equations to an algebraic set of equations is the Gauss-Seidel method which can be solved numerically with an over-relaxation on process at different Rayleigh numbers. The Matlab program [10] solves the governing equations at each node in the face until reaching the following convergence condition:

$$\left|\frac{max\theta^m - max\theta^{m+1}}{max\theta^{m+1}}\right| < 10^{-6} \qquad (30)$$

where θ represents the variable and the superscript $m+1$ is the current iteration and m is the previous iteration.

Mesh independency test

Reliable numerical solutions are obtained by performing a mesh convergence study using the Matlab code. This is done by changing the size of elements mesh un-

til the numerical results converge to a table value which is mesh independent. Figure 3 shows the variation of maximum velocity (V_{max}) versus element mesh size and variation of minimum stream function (Ψ_{min}) versus element mesh size. Figure 4 shows the variation of maximum temperature (θ_{max}) versus element mesh size for Rayleigh number value ($Ra = 10^4$).

The numerical simulations were performed for nine different element sizes of 0.005, 0.006, 0.007, 0.008, 0.009, 0.01, 0.02, 0.03 and 0.04. Finally, the mesh size is independent for element sizes of 0.01. Further reduction of the element size below 0.01 doesn't change the numerical results.
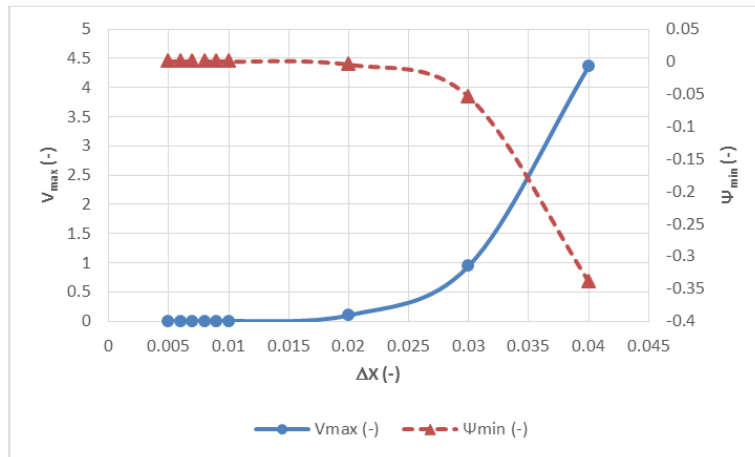
Fig. 3 Variation of maximum velocity and minimum stream function versus element mesh size
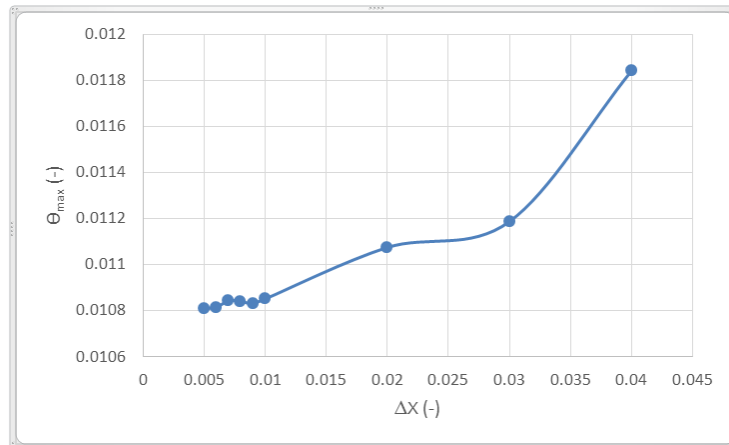
Fig. 4 Variation of maximum temperature versus element mesh size

Model Validation

In order to verify the accuracy of the numerical code, comparisons with the previously published results are necessary. The present numerical code is verified against a documented numerical study. The governing equations are solved for a Prandtl number, Pr=0.7. The solutions are obtained for a Rayleigh number of 10^4. The Pr and Ra are chosen such that the direct comparison is possible with the solution of Tahar and Mahfoud [6]. The isotherms and streamlines are compared with results of [6] in Figures 5 and 6, respec-

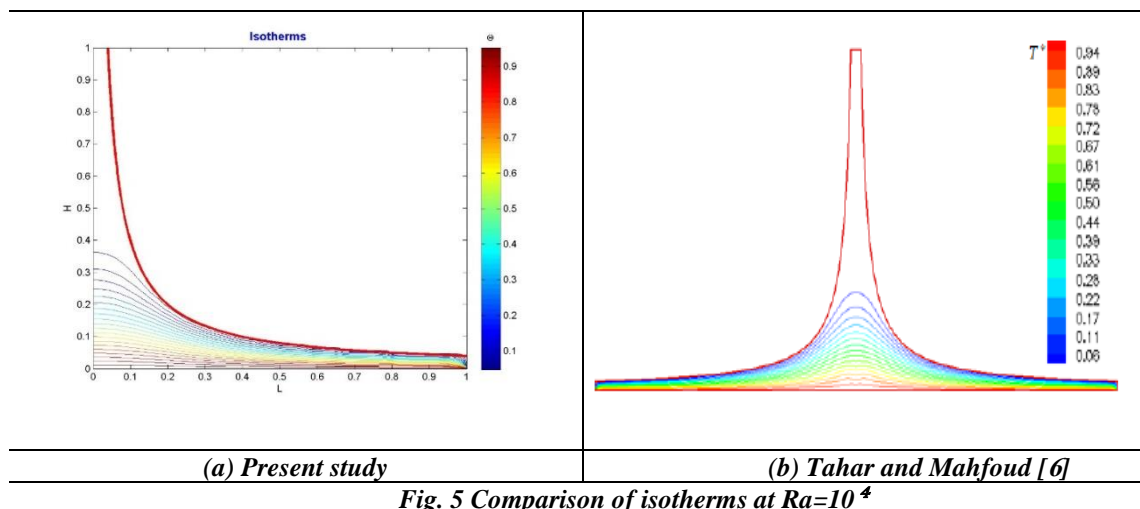tively. It is observed that the present results are in good agreement with previous nu-

merical work.

| *(a) Present study* | *(b) Tahar and Mahfoud [6]* |

Fig. 5 Comparison of isotherms at Ra=10^4

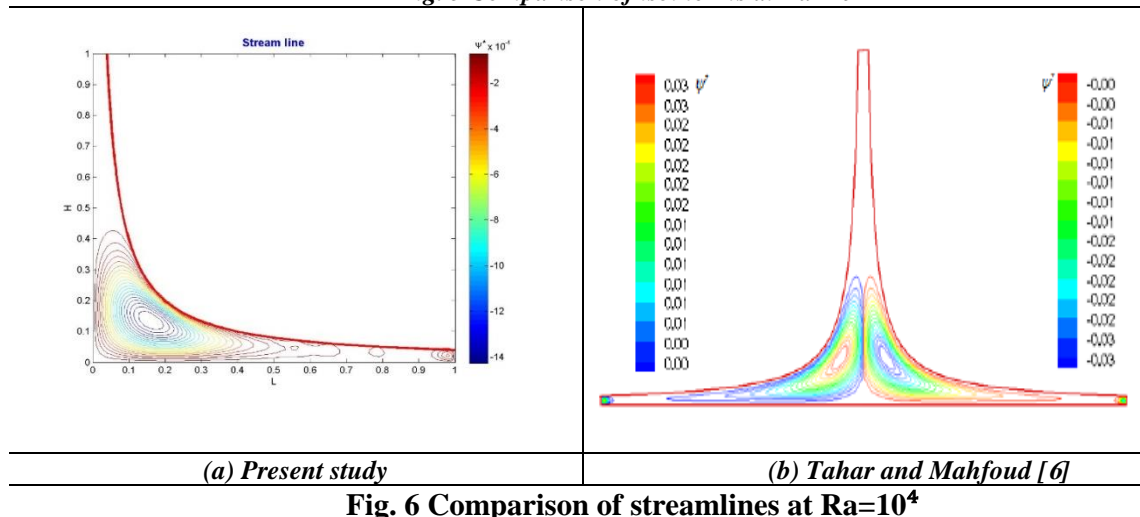| *(a) Present study* | *(b) Tahar and Mahfoud [6]* |

Fig. 6 Comparison of streamlines at Ra=10^4

Our objective is to analyse the effect of geometry on heat transfer and flow of air into the chimney. For this reason, the isotherms and streamlines are presented in different geometries for three different Rayleigh numbers and inlet velocities to illustrate what happens inside the solar chimney when changing any one of these factors and present the corresponding streamlines and the isotherms inside the chimney.

Effect of Rayleigh number (Ra)

Figures 7 and 8 show the distribution of streamlines and isotherms for solar chimney at Ra = 10^3 and 10^6 for Y/X =0.5

and U_{in}= 0.01. As is to be expected, with low Ra, streamlines are parallel to the arc line of chimney and there are no vortices. This is the result that the buoyancy force overcomes the friction force. The increase in Ra (Ra=10^6) creates vortices in streamlines in the collector area, Fig. 8. The presence of counter rotating vortices in the centre of the collector (Fig. 8) is due to the symmetrical structure of the chimney favouring the upward flow (the particles of the fluid move upwards, under the action of buoyancy force) indicates the presence of resistance of friction and gravity forces against the forces of buoyancy. Figure 8 shows the vortices which result from friction forces against the forces of buoyancy. So, the increase in the Ra causes vortices in streamlines while deformation in iso-
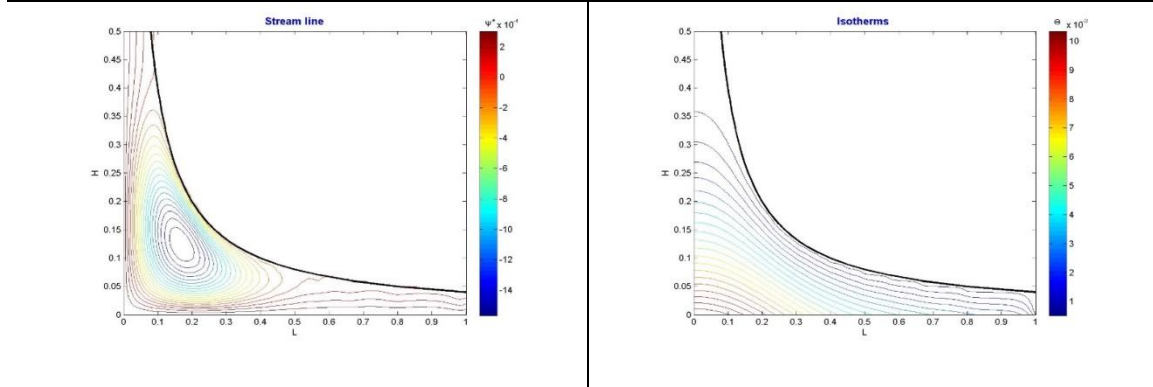
thermal lines because of the change in streamlines which result in the dispersion

of heat inside the chimney.
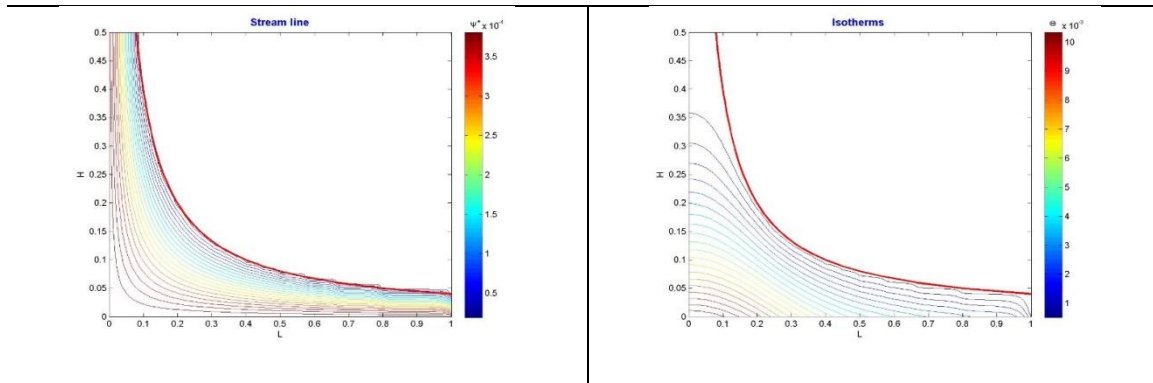
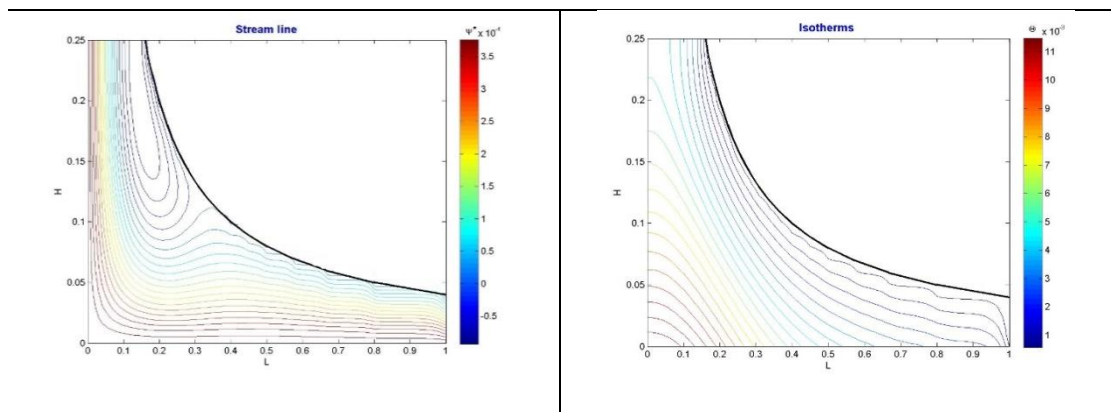*Fig. 7 Streamlines and isotherms for Ra=10³ at Y/X=0.25 and U$_{in}$=0.01*

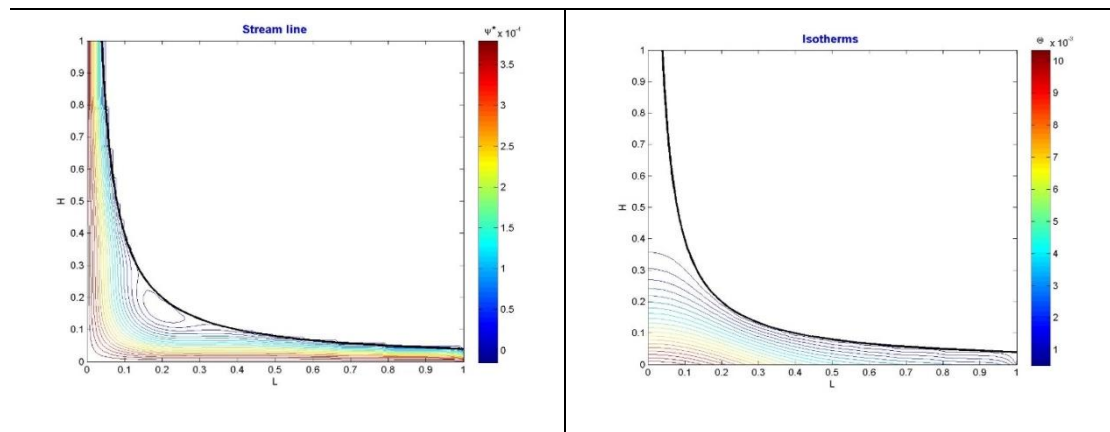*Fig. 8 Streamlines and isotherms for Ra=10 ⁶ at Y/X=0.25 and U$_{in}$=0.01*

Effect of aspect ratio (Y/X)

Figures 9 and 10 show the distribution of streamlines and isotherms for solar chimney at Y/X = 0.25 and 1 for Ra =10^5 and U$_{in}$= 0.01. An increase in the Y/X causes vortices in streamlines at distance near inlet of chimney because the increase of friction force over buoyancy force helps the flow to exit from the chimney as lami-

nar form. Also, the increase in the ratio Y/X causes the high isothermal lines to stay in the chimney. The temperature at exit is nearest to the ambient temperature led to no change in density, the later prevented the occurrence of fluid flow and back flow as indicated from the streamlines, Fig. 10.

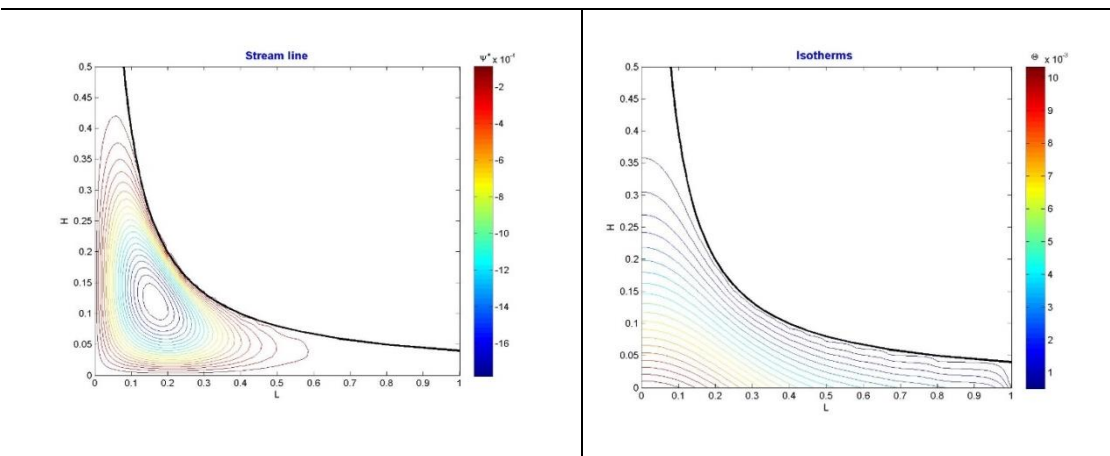*Fig. 9 Streamlines and isotherms for Ra=10 ⁵ at Y/X=0.25 and U$_{in}$=0.01*

Fig. 10 Streamlines and isotherms for Ra=10 ^{5} at Y/X=1 and U$_{in}$=0.01

Effect of inlet velocity (U$_{in}$)

Figures 11 and 12 show the distribution of streamlines and isotherms for solar chimney at U$_{in}$=0 and 0.5 for Ra =10^6 and Y/X =0.5. The decrease in the inlet velocity (U$_{in}$=0) causes vortices in streamlines to be formed, whereas increasing the inlet velocity (U$_{in}$=0.5), the parallel flow exit from the chimney and vortices in chimney decrease which indicate increase in buoyancy force. The increase in the U$_{in}$ causes the streamlines exit from chimney led to increase heating in chimney, it's not favour because refer to heat dissipated in ambient and do not benefit with it in heating collector.

*Fig. 11 Streamlines and isotherms for Ra=10 ^{6} at Y/X=0.5 and U$_{in}$=0*
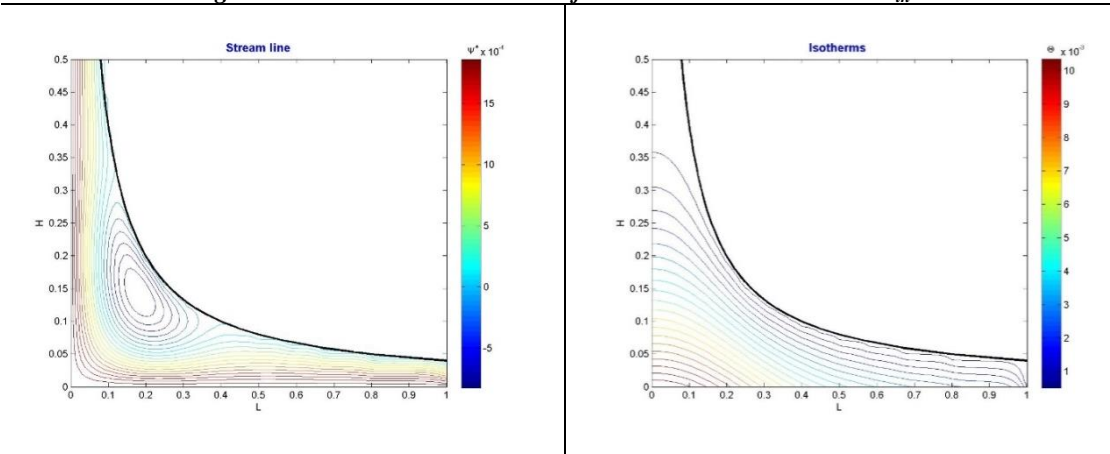
Fig. 12 Streamlines and isotherms for Ra=10 ^{6} at Y/X=0.5 and U$_{in}$=0.5

Application in city in Egypt

Figure 13 shows the monthly averaged midday insolation incident on a horizontal surface measured by NASA in New Vellage city in Egypt, which is used for the calculations of average monthly power generation, El-Haroun [11]. The expected average monthly power output using chimney with scale L=2000m, H=1000m is given in Fig. 13. The generated power in spring and summer months is found to be higher than its value in other months. The generated power from this location reaches its maximum value between 11 and 24 MW in June. Therefore, a part of energy demand in Egypt can be covered through the use of solar chimney power plants. This reduces the use of conventional sources of energy, like oil and natural gas, which is considered the main source of the emissions of harmful gases and expenses. The world will use this technology in future to meet the need for electrical energy.
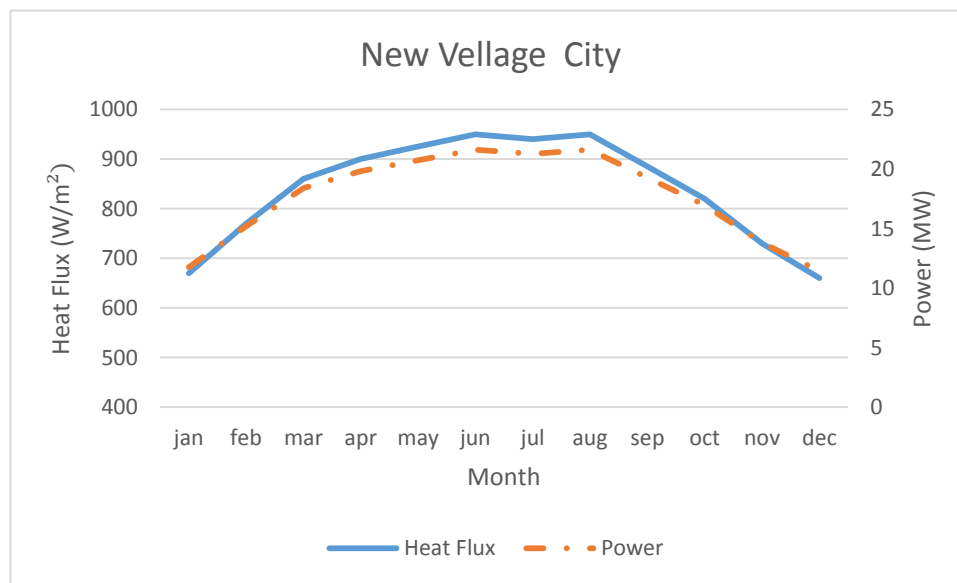
Fig. 13 Average monthly solar radiation intensity and power in New Village city

Conclusions

The main objective of this study is to investigate the performance of a solar chimney power plant. A validated numerical simulation of the solar chimney has been developed by comparison between the numerical and published simulation. The model has been used to predict of performance of solar chimney power plant in Egypt.

The following conclusions can be drawn from this study:

1. Increasing the Rayleigh number leads to forming vortices in the chimney but when decreasing the Rayleigh number makes the flow in chimney laminar and parallel to the arc of collector. Increasing the aspect ratio helps in the formation of vortices in the chimney because of the increase of friction force over buoyancy force.

2. Increasing inlet velocity helps buoyancy force to overcome vortices which formed, and led to the flow became laminar, also affects in the increase of the maximum velocity in the chimney.

3. The weather conditions of Egypt such as solar radiation intensity and inlet air velocity are encouraging to produce clear power by using solar chimney.

Reference

[1.] W. Haaf, K. Friedrich, G. Mayr, and J. Schlaich, "Solar Chimneys, Part I: Principle and Construction of the Pi-

lot Plant in Manzanares", International Journal of Solar Energy, Vol. 2, pp. 3-20, 1983.

[2.] J. Schlaich, R. Bergermann, W. Schiel, and G. Weinrebe, "Design of Commercial Solar Updraft Tower Systems-Utilization of Solar Induced Convective Flows for Power Generation", Journal of Solar Energy Engineering, Vol. 127, No. 1, pp. 117-124, 2005.

[3.] X. Zhou, J. Yang, B. Xiao, and G. Hou, "Simu-lation of a Pilot Solar Chimney Thermal Power Generating Equipment", Renewable Energy, Vol. 32, No. 10, pp. 1637-1644, 2007.

[4.] M. A. dos Santos Bernardes, R. Molina Valle, and M. F.-B. Cortez, "Numerical Analysis of Natural Laminar Convection in a Radial Solar Heater", International Journal of Thermal Sciences, Vol. 38, No. 1, pp. 42-50, 1999.

[5.] [5] H. Huang, H. Zhang, Y. Huang, and F. Lu, "Simulation Calculation on Solar Chimney Power Plant System", in Challenges of Power Engineering and Environment, Springer Berlin Heidelberg, 2007, pp. 1158-1161.

[6.] T. Tahar and D. Mahfoud, "Numerical Simulation of Natural Convection in a Solar Chimney", International Journal of Renewable Energy Research, Vol. 2, No. 4, pp. 712-717, 2011.

[7.] A. A. Mostafa, M. F. Sedrak, and A. M. Abdel Dayem, "Performance of a Solar Chimney under Egyptian Weather Conditions: Numerical Simulation and Experimental Validation", Energy Science and Technology, Vol. 1, No. 1, pp. 49-63, 2011.

[8.] M. O. Hamdan, "Analysis of Solar Chimney Power Plant Utilizing Chimney Discrete model", Renewable Energy, Vol. 56, pp. 50-54, 2013.

[9.] F. Cao, H.S. Li, L. Zhao, T.Y. Bao and L.J. Guo , "Design and Simulation of the Solar Chimney Power Plants with TRNSYS", Solar Energy, Vol. 98, Part A, pp. 23–33, 2013.

[10.] Matlab 2012 b, http://www.mathworks.com/downloads/

[11.] A.A. El-Haroun, "Performance Evaluation of Solar Chimney Power Plants in Egypt", International Journal of Pure and Applied Sciences and Technology, Vol. 13 (2), pp. 49-59, 2012.